Journal of Zhejiang University SCIENCE A
ISSN 1009-3095 (Print); ISSN 1862-1775 (Online)
www.zju.edu.cn/jzus; www.springerlink.com
E-mail: jzus@zju.edu.cn

DVB-S2 inner receiver design for broadcasting mode

YANG Jian-xiao[†1], WANG Kuang[1], ZOU Zhi-yong[2]

([1]*Institute of Information Science and Electronic Engineering, Zhejiang University, Hangzhou 310027, China*)

([2]*Guoxin Co. Ltd, Hangzhou 310027, China*)

[†]E-mail: shawn_yangjx@hotmail.com

Received Mar. 10, 2006; revision accepted Sept. 4, 2006

Abstract: This paper details on the design of DVB-S2 receivers which is compliant with the broadcasting mode. Special attention is paid to the specific receiver functions necessary to demodulate the received signal. To show the system performance we consider the design of a complete receiver consisting of timing recovery unit, frame synchronization unit, frequency recovery unit and phase recovery unit. The system is easier to hardware implementation comparing with that provided in (ETSI, 2005; Sun *et al*., 2004). After the performance of the algorithms is analyzed and a quantitative result is given, this allows us to draw conclusions concerning the achievable system performance under realistic complexity assumptions.

Key words: DVB-S2, Timing recovery, Frame synchronization, Frequency recovery, Phase recovery
doi:10.1631/jzus.2007.A0028 **Document code:** A **CLC number:** TN93

INTRODUCTION

The second generation satellite digital video broadcasting standard (ETSI, 2004) has come out recently. Compared with the previous satellite standard DVB-S (ETSI, 2003), DVB-S2 has more advantages, such as the 30% increase in channel capacity, the more reliable performance, and the more efficient usage of transponders. The DVB-S2 standard has been designed having in mind the peculiarities of the satellite channel, particularly the link fading impairments and the carrier phase noise (Nemer, 2005) dominated by the user terminal RF front-end.

The most challenging issues that one has to deal with when designing a DVB-S2 demodulator are the rapid frame synchronization and the carrier recovery unit. In broadband satellite transmission, the phase of the carrier is usually affected by a number of distortions (Casini *et al*., 2004). Many algorithms are available in the literature to address the issue of carrier phase recovery (Mengali and D'Andrea, 1997) for different modulation schemes. However, using low cost commercial low noise blocks (LNBs) and tuners leads to a remarkable increase of the carrier phase noise which the system has to be able to tolerate making conventional carrier phase estimators suffer from an unacceptable cycle slip rate.

The rest of the paper is organized as follows. We introduce the structure of the physical layer frame in the second section. In the third section, we propose a digital inner receiver scheme and the accompanying problems of each part. In the fourth section, through researching the algorithms in the key units of the inner receiver, we give out the algorithms of the timing synchronization unit, the frame synchronization unit, and the carrier recovery unit. In the fifth section, the performance of each unit is analyzed by means of fixed point simulation. We make the conclusion in the final section.

Physical layer framing

The DVB-S2 physical layer frame (named PLFRAME) structure shown in Fig.1 is critical in the design of the synchronization algorithms. The frame is well explained as follows. XFECFRAME (length: 64800 bits for broadcasting mode) is the data frame after inner and outer coding. After mapping, XFECFRAME is sliced into an integer N of constant

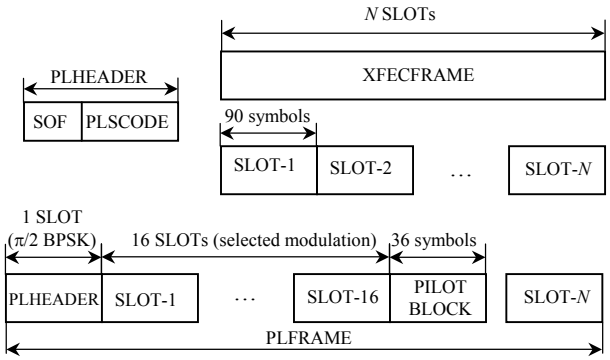

Fig.1 PLFRAME structure

length SLOTs (length: 90 symbols each). The physical layer frame header (named PLHEADER) is composed of an SOF field (26 symbols, identifying the Start of Frame) and a scrambled and coded PLSCODE field (64 symbols, identifying the physical layer transport information) which will be modulated into π/2 BPSK symbols. The PLFRAME can be configured with or without pilot modes. In the former case a PILOT BLOCK shall be composed of 36 pilot symbols. The first PILOT BLOCK shall be inserted 16 SLOTs after the PLHEADER, the second after 32 SLOTs and so on.

PROBLEM STATEMENT

After AGC, the received signal can be expressed as

$$r(t) = a_0 s(t) \exp(\mathrm{j}2\pi f_c t) + n(t), \tag{1}$$

where a_0, $s(t)$, f_c and $n(t)$ denote the complex amplitude factor, the base-band modulated signal, the residual carrier frequency offset and the additive white Gaussian noise respectively. By sampling we get the discrete signal in the time $t_k=kT$,

$$r(k) = a_0 s(k) \exp(\mathrm{j}2\pi f_c kT) + n(k), \tag{2}$$

where T is the symbol duration, $s(k)=A\exp(\mathrm{j}\theta_k)=I_k+\mathrm{j}Q_k$, and A is the amplitude of the symbol.

As shown in Fig.2, the DVB-S2 demodulator we proposed consists of a timing synchronization unit, a frame synchronization unit, a carrier frequency detector loop and a carrier phase detector loop.

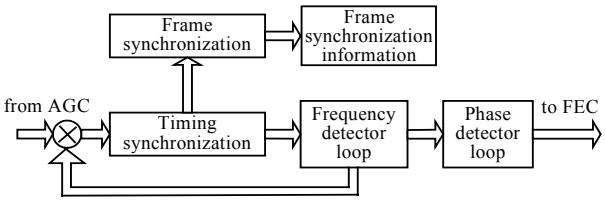

Fig.2 Inner receiver architecture of DVB-S2

Timing synchronization

We adopt Gardner TED algorithm (Gardner, 1986) in timing error detector. This algorithm is non-data aided and is insensitive to carrier phase error. The expression of the algorithm is

$$\begin{aligned} e(t) = {} & I(t-T/2)[I(t)-I(t-T)] \\ & + Q(t-T/2)[Q(t)-Q(t-T)], \end{aligned} \tag{3}$$

where $I(t)$ and $Q(t)$ denote the real part and the imaginary part of the received signal, respectively.

As we know, the performance of this algorithm is sensitive to the carrier frequency error. The timing error with nonzero frequency error should be modified as

$$\begin{aligned} e(t) = {} & \{I(t-T/2)[I(t)-I(t-T)] \\ & + Q(t-T/2)[Q(t)-Q(t-T)]\}\cos(2\pi f_c T) \\ & - \{I(t-T/2)[Q(t)+Q(t-T)] \\ & - Q(t-T/2)[I(t)+I(t-T)]\}\sin(2\pi f_c T). \end{aligned} \tag{4}$$

The timing error spectrum before the loop filter is shown in Fig.3. Just as shown, the Gardner TED algorithm suffers from a slightly higher self-noise caused by the sin terms in Eq.(4) and also suffers from the systematic timing phase jitter caused by the fact that intermediate samples do not only depend on both adjacent data symbols but on all data samples.

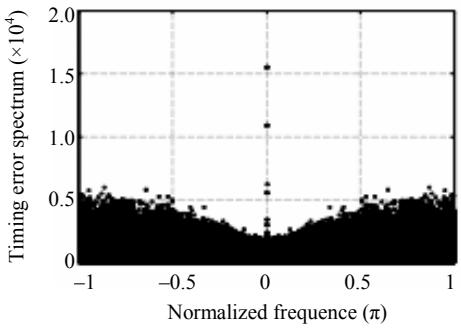

Fig.3 Timing error spectrum without pre-filtering

Frame synchronization

Frame acquisition in DVB-S2 suffers from two major impairments: the extremely low SNR, which can indeed assume negative values in dB, and the unknown carrier frequency offset and phase. In addition, at terminal startup the uncertainty region equals the entire frame length, TF, which in the worst case is as large as 33282 QPSK symbols. At first glance, one could hope to improve performance by exploiting multi-dwell procedures (i.e., collecting information from multiple frames before making a final decision). Unfortunately, this approach cannot be used in DVB-S2, where the frame length depends on the selected coding and modulation pair. In particular, the frame format is signaled to the receiver by a 64-symbol physical layer signaling (PLS) field and the PLS field cannot be decoded accurately prior to frame synchronization.

Frequency recovery unit

Frequency recovery is also one of the most critical units due to the fact that DVB-S2 mass market terminals will typically incorporate low-cost oscillators (the terminal LNB oscillator instabilities) and Doppler effects, which introduce large initial frequency offsets (e.g., 5 MHz at 27.5 Mbaud).

Phase recovery unit

The carrier phase recovery algorithm has to cope with a residual carrier frequency error from the carrier frequency recovery unit as well as a strong phase noise caused by the terminal LNB RF oscillator.

INNER RECEIVER ISSUES

Timing synchronization

In this paper, we propose an IIR pre-filter scheme. Comparing with the pre-filter put before the TED in (D'Andrea and Luise, 1993; 1996), we put the pre-filter between the TED and the loop filter. We do not propose higher order filter because the 1st order loop filter is enough to suppress the noise and make both loop robustness and the loop filter parameters easily configurable. And the timing error spectrum after pre-filtering is shown in Fig.4.

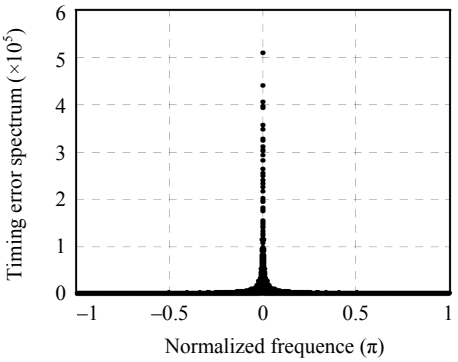

Fig.4 Timing error spectrum with pre-filtering

Just as shown in Fig.3, the timing error focuses most information on the low frequency range while the noise focuses on the high frequency range. So the key parameter of the pre-filter is the bandwidth. After the bandwidth has been properly chosen, most information on the timing error has been reserved and most parts of the noise have been suppressed as shown in Fig.4.

Frame synchronization

A differential correlation based frame synchronization algorithm is given in (ETSI, 2005), in which the total 57 correlation information is utilized (including 25 correlations in SOF field and 32 correlations in PLSCODE field).

Under low SNR environment, the algorithm proposed in (ETSI, 2005) generates many pseudo peaks which are shown in Fig.9 and turns out to be too short to provide reliable convergence at low SNRs by using the 57 correlations.

Since the SOF is known, and only the information on adjacent correlation is used, SOF information was not utilized sufficiently. In this paper, we strengthen the former algorithm by using the structure shown in Fig.5 with the detection expression being shown in Eq.(5):

$$\begin{cases} location = \arg\limits_{n}\{\max[sum(n)]\}, \\ sum(n) = \sum\limits_{l=1}^{L}\left\{\left|\sum\limits_{m=0}^{M-1-l} r(n+m+l)r^*(n+m)c(m,l)\right| \right. \\ \qquad \left. + \left|\sum\limits_{i=0}^{P-1} r(n+M+2i+1)r^*(n+M+2i)c(l)\right|\right\}, \end{cases} \quad (5)$$

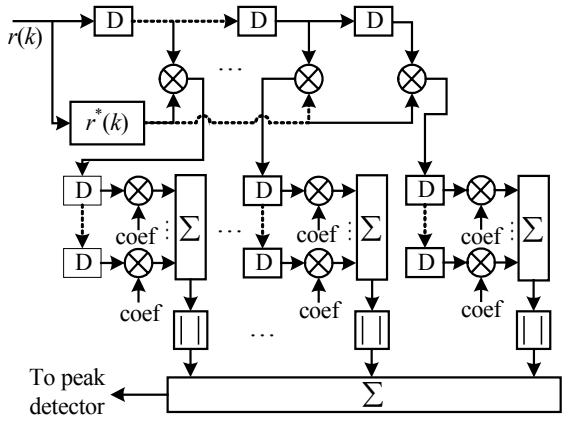

Fig.5 Frame synchronization detector

where M is the SOF length which is 26, P is the length of PLSCODE which is 64, $c(m,l)$ denotes the taps of the differential correlation, L is the maximum correlation interval. Compared with the proposed algorithm in (ETSI, 2005), the computation complexity increases with L. The taps associated with shift register for computing the correlation should follow these steps:

(1) Set all the registers to zero.

(2) Shift the modulated SOF and a modulated and scrambled code word of PLSCODE into the circuit.

(3) Once the lowest registers become nonzero, the tap associated with a register is just the complex conjugate of the coef.

Given that the modulated SOF and PLSCODE take only ±1, ±j, the taps only take these four possible values as well. Obviously, if L=1, the algorithm we propose reduces to the one given in (ETSI, 2005).

The output is then further processed by a peak search algorithm. The conventional approach is to compare the output correlation sum with a predetermined threshold. If the value is larger than the threshold, it is a possible PLHEADER location and can be called the candidate. And the post verification is based on the detection of the location at a distance L_s which belongs to the set {32490, 33282, 21690, 22194}. Comparing with the strategy proposed in (Sun *et al*., 2004), we do not utilize the PLSC to verify that the PLSC can tolerate large noise but is very sensitive to the carrier frequency offset (the range is less than $2.5\times10^{-3}f_s$), especially, while the frequency carrier recovery unit is preceded by the frame synchronization, the residual frequency offset is much higher than $2.5\times10^{-3}f_s$.

Frequency recovery

Many algorithms have been designed for frequency detector (FD), e.g. the maximum-likelihood based Gardner frequency detector (GFD) proposed in (Gardner, 1990) and the reduced version reduced complexity frequency detector (RCFD) (Karam and Sari, 1995). These two algorithms need modification of the matched filter, which will increase the complexity and hardware expense. The algorithm proposed in (Mengali and D'Andrea, 1997) can only utilize 26 information symbols in SOF field and is constrained by the number of the information symbols per-frame; it will spend more time to reach the frequency synchronization.

In this paper we propose a novel FD algorithm which does not require the PLHEADER information. The only required information is the position of the PLHEADER with the derivation of the algorithm being shown below.

Suppose $tr(k)=a_0s(k)\exp(j2\pi f_c kT)$, where $tr(k)$ is the transmission signal, the difference between the adjacent symbols $s(k)$ and $s(k-1)$ is $\pm\pi/2$ caused by the $\pi/2$ BPSK modulation, we have

$$\begin{aligned}\mathrm{Im}\{tr^2(k)[tr^2(k-1)]^*\} &= \mathrm{Im}\{-A^4\exp(4\pi f_c T)\}\\ &= -A^4\sin(4\pi f_c T),\end{aligned} \tag{6}$$

where Im{} and []* denote imaginary part and conjugate, respectively.

Modified $tr(k)=a_0s(k)\exp(j2\pi f_c kT)+n(k)$, and denote $n(k)=n_I(k)+jn_Q(k)$, the term $tr^2(k)$ can be extended as follows:

$$\begin{aligned}tr^2(k) &= [a_0s(k)\exp(j2\pi f_c kT)]^2 + n^2(k)\\ &\quad + 2n(k)a_0s(k)\exp(j2\pi f_c kT)\\ &= [a_0s(k)\exp(j2\pi f_c kT)]^2 + \{[n_I^2(k)-n_Q^2(k)]\\ &\quad + 2jn_I(k)n_Q(k) + 2n(k)a_0s(k)\exp(j2\pi f_c kT)\}.\end{aligned} \tag{7}$$

Useful output of the algorithm is the loop filter output which equals the average over many samples, not the value of an isolated sample, then the noise generated by the marked terms will be filtered out, whose remaining term is of the form

$$\begin{aligned}Avg\{tr^2(k)[tr^2(k-1)]^*\} &= Avg\{tr^2(k)\}Avg\{[tr^2(k-1)]^*\}\\ &= -A^4\exp(4\pi f_c T).\end{aligned} \tag{8}$$

Based on Eq.(6), the frequency detection error yields

$$E\{e(k)\} = E\{\mathrm{Im}[r^2(k)[r^2(k-1)]^*]\} = -A^4 \sin(4\pi f_c T), \quad (9)$$

where $r(k)$ is the received signal after AGC, and A is the amplitude of the symbol.

The frequency acquisition range is equal to the range of the algorithm given in (Mengali and D'Andrea, 1997), but the frequency error information accuracy of the new algorithm can be greatly improved and does not require any information symbol.

With PILOT and PLHEADER information being utilized, the convergence speed can be greatly improved. And the number of training symbols increases up to 90, which increases the accuracy and the robustness of the estimation.

Phase recovery

The MPSK modulated signal can be demodulated using M-power Costas loop, which can increase the hardware expense greatly when M is large. A feed-forward maximum-likelihood phase compensation based algorithm is proposed by Sun *et al*.(2004). But the algorithm can work only if the residual frequency offset is lower than $3.5\times10^{-4}f_s$ after FD which is difficult for FD unit to reach such a criterion at low SNR.

In this paper, the polarity-type Costas loop has been adopted by van der Wal and Montreuil (1995) and Huang *et al*.(2004), whose expression is

$$e(t)_{\mathrm{QPSK}} = \mathrm{sgn}[I(t)]Q(t) - \mathrm{sgn}[Q(t)]I(t). \quad (10)$$

But it is only suitable for QPSK. The modifications must be done for 8PSK as follows

$$e(t)_{8\mathrm{PSK}} = \begin{cases} -\mathrm{sgn}[Q(t)]I(t), & \text{if } |Q(t)| > 2.414|I(t)|, \\ \mathrm{sgn}[I(t)]Q(t), & \text{if } |Q(t)| < 0.414|I(t)|, \\ \mathrm{sgn}[I(t)]Q(t) - \mathrm{sgn}[Q(t)]I(t), & \text{else.} \end{cases} \quad (11)$$

We also present further modifications to the above algorithm as shown below. Denote $S_I=I^2(t)-Q^2(t)$ and $S_Q=2I(t)Q(t)$, we yield that

$$e(t)_{\mathrm{QPSK}}=\mathrm{sgn}(S_Q)S_I, \quad (12)$$

$$e(t)_{8\mathrm{PSK}} = \begin{cases} \mathrm{sgn}(S_I)\cdot S_Q, & \text{if } |S_I| > |S_Q|, \\ \mathrm{sgn}(S_Q)\cdot S_I, & \text{else.} \end{cases} \quad (13)$$

We do not adopt high power phase recovery algorithm, which can not only greatly increase the hardware expense, but also be a high energy consumption solution. Since the low energy consumption design is one of the most critical parts in DVB-S2 scheme, lower power less than 2 is an optimization solution.

SIMULATION RESULTS

Timing synchronization

The timing errors after loop filtering with and without pre-filtering are shown in Fig.6 and Fig.7 respectively. The jitter in Fig.6 has been greatly decreased and the pre-filtering has effectively suppressed the noise. In our simulation, pre-filtering bandwidth being 5~6 times that of the loop filter bandwidth is optimal. Fig.8 shows the performance of the timing synchronization in terms of the RMS of the residual timing frequency error.

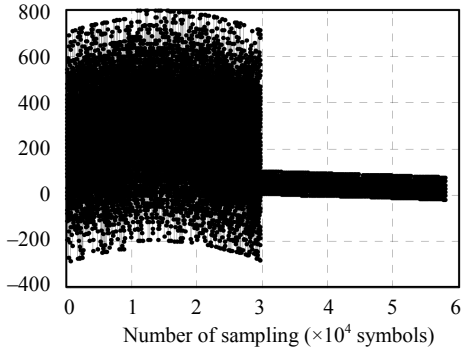

Fig.6 LPF output without pre-filtering

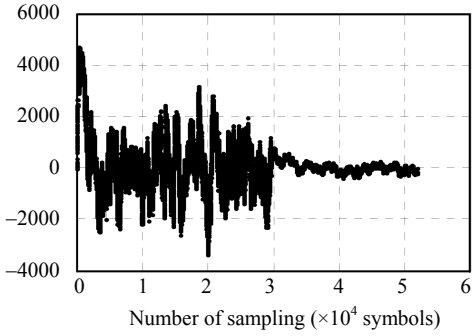

Fig.7 LPF output with pre-filtering

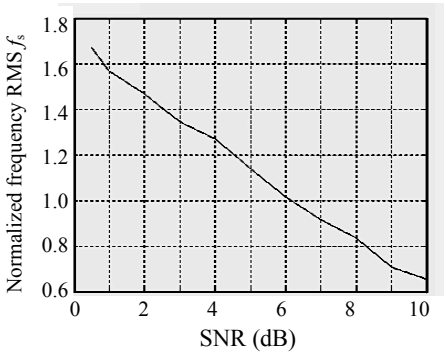

Fig.8 Performance of timing synchronization

Frame synchronization

In Eq.(5), the parameter L should be properly selected. With the increase of L, performance of the candidate frame synchronization algorithm can be greatly increased. But considering the hardware expense, there should be tradeoff between the performance and the expense. In our simulation, we choose 7. Performance of the candidate is shown in Fig.9. The simulation is performed with 1.0 dB SNR and $0.2f_s$ (the maximum tolerable frequency offset of the Gardner timing algorithm) residual frequency offset.

Extensive computer simulations have been performed. Table 1 summarizes the mean time and the time with 99.9% confidence to acquire frame synchronization under the environment with 1 M symbol rate, –0.5 dB E_s/N_0 and $0.2f_s$ carrier frequency offset.

Table 1 Time to frame synchronization

Modulation	Method	Mean time (ms)	Time with 99.9% confidence (ms)
QPSK	SOF	250	512
QPSK	SOF+PLSC	182	406
8PSK	SOF	262	532
8PSK	SOF+PLSC	196	420

Table 2 gives the mean time to acquire frame synchronization under environment with –2 dB E_s/N_0 and different symbol rates. It shows clearly that by sufficiently utilizing the PLHEADER, the acquiring time can be greatly shortened. Comparing with the performance proposed by Sun *et al*.(2004), significant improvement has been obtained.

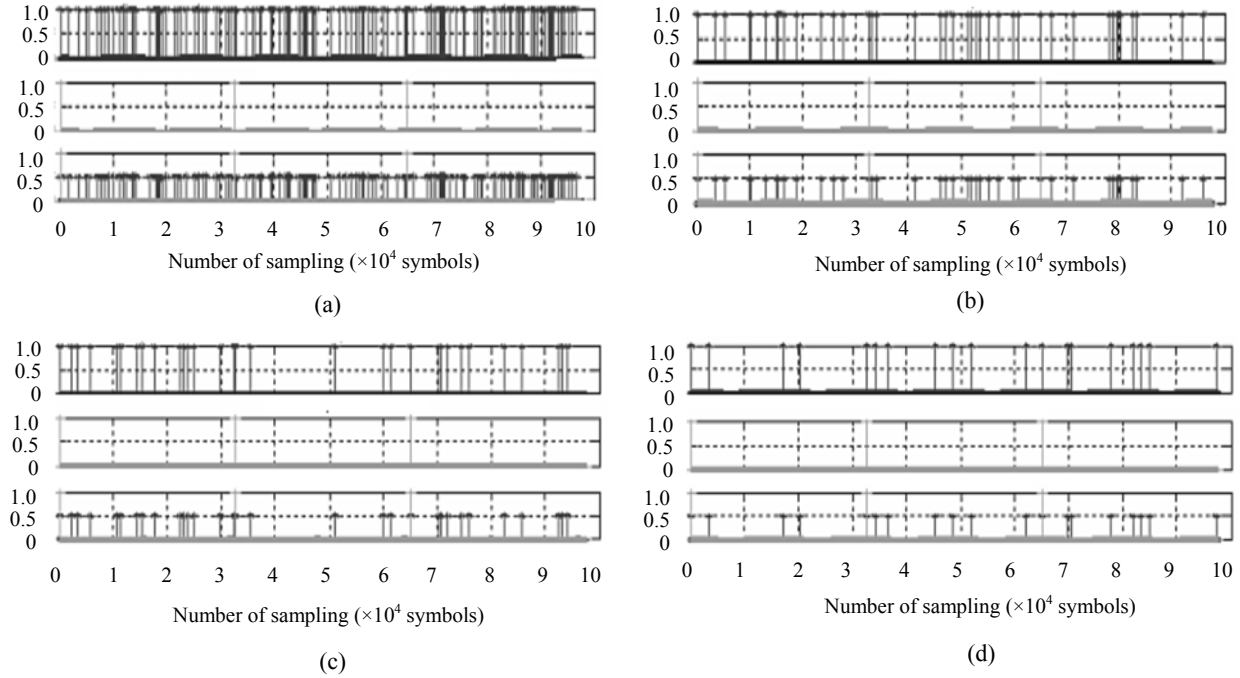

Fig.9 Candidate algorithm performance with different *L*'s. (a) *L*=1; (b) *L*=3; (c) *L*=5; (d) *L*=7
Middle subfigures and top subfigures denote the correct and the candidate positions, respectively. Bottom subfigures are the ones combined with the correct position (amplitude is 1.0) and candidate position (amplitude is 0.5)

Table 2 Time to frame synchronization with different symbol rates

Modulation	Method	Mean time (ms)	Time with 99.9% confidence (ms)
QPSK	SOF	21.5	76.9
QPSK	SOF+PLSC	19.3	56.5
8PSK	SOF	23.2	80.3
8PSK	SOF+PLSC	20.7	61.2

Frequency recovery

Computer simulations were conducted to test the carrier recovery algorithm for pilotless modes in the presence of strong AWGN and the phase noise specified by DVB-S2. The received signal has a 25 M symbol rate and a 5 M frequency offset. Fig.10 shows the RMS frequency error of the FD unit operating on QPSK frames in the pilotless mode. Autocorrelation is accumulated only on 57-symbol PLHEADER. At –2 dB, the RMS error is $1.2\times10^{-4}f_s$ over 20 frames.

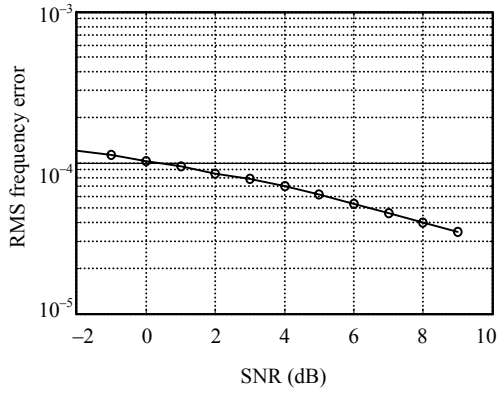

Fig.10 Performance of frequency recovery unit

Phase recovery

The phase error and the residual frequency offset can be cancelled by PFD loop after the FD loop locks. Under the condition of AWGN, we should consider the tradeoff between the convergence speed and the stability error, including the capability of combating the white noise and the phase noise. We adopt Eqs.(10), (11) and Eqs.(12), (13) into acquisition process and tracking process respectively. Furthermore, in each modulation mode, there are two sets of filter parameters for the acquisition process and the tracking process respectively. Table 3 summarizes the performance of the phase recovery algorithm with phase noise and without pilots.

Table 3 Phase recovery performance

Mode	SNR (dB)	RMS (°)	Cycle-slip rate
QPSK	0.3	3.18	$<10^{-8}$
8PSK	5.0	3.05	$<10^{-8}$

System performance

The ultimate goal of the receiver design is not to degrade the performance of direct decision when compared with ideal AWGN channel. The curves of the QPSK and 8PSK SER vs SNR are shown in Fig.11 and Fig.12 respectively. It can be easily seen that the SER curve of the simulation results approaches the theoretical one, especially at low SNR. But with the increase of the SNR, the simulation SER curve departs from the theoretical one because of the quantization precision.

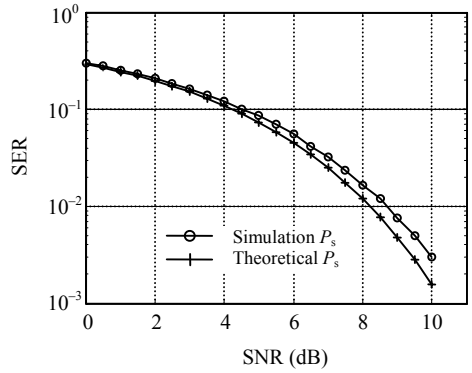

Fig.11 QPSK SER vs SNR

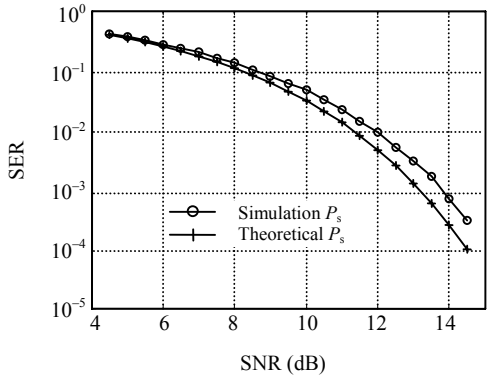

Fig.12 8PSK SER vs SNR

The inner receiver connected with the LDPC decoder was extensively simulated to verify the final performance. The performance of MPEG PER (packet error rate) in the presence of the phase noise in AWGN channel is shown in Fig.13 and Fig.14.

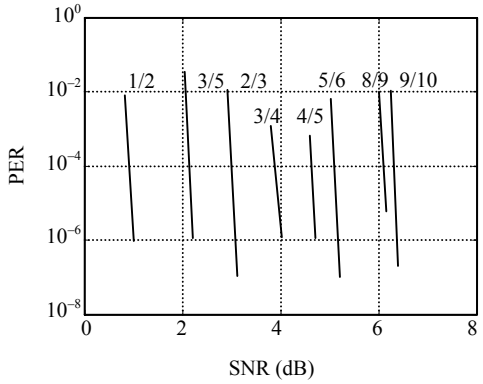

Fig.13 Performance of QPSK

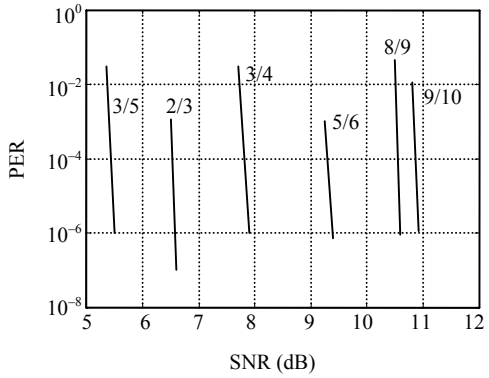

Fig.14 Performance of 8PSK

CONCLUSION

In this paper we have considered the systematic design of inner receiver algorithms for DVB-S2 based transmission systems. Taking into account the physical layer frame structure of the DVB-S2 scenario, we have derived algorithms with close-to-optimum performance while providing robust and fast acquisition. Simulation results showed that the receiver does not degrade the performance when compared with ideal AWGN channel.

References

Casini, E., de Gaudenzi, R., Ginesi, A., 2004. DVB-S2 modem algorithms design and performance over typical satellite channels. *Int. J. Satell. Commun. Network.*, **22**(3):281-318. [doi:10.1002/sat.791]

D'Andrea, N.A., Luise, M., 1993. Design and analysis of a jittter-free clock recovery scheme for QAM systems. *IEEE Trans. Commun.*, **41**(9):1296-1299. [doi:10.1109/26.237846]

D'Andrea, N.A., Luise, M., 1996. Optimization of symbol timing recovery for QAM data demodulators. *IEEE Trans. Commun.*, **44**(3):399-406. [doi:10.1109/26.486334]

ETSI, 2003. EN300 421 v.1.1.2 Digital Video Broadcasting (DVB): Framing Structure, Channel Coding and Modulation for 11/12 GHz Satellite Services.

ETSI, 2004. EN302 307 v1.1.1 Digital Video Broadcasting (DVB): Second Generation Framing Structure, Channel Coding and Modulation Systems for Broadcasting, Interactive Services, News Gathering and Other Broadband Satellite Application.

ETSI, 2005. TR 102 376 v1.1.1 Digital Video Broadcasting (DVB): User Guidelines for the Second Generation System for Broadcasting, Interactive Services, News Gathering and Other Broadband Satellite Application.

Gardner, F.M., 1986. A BPSK/QPSK timing-error detector for sampled receivers. *IEEE Trans. Commun.*, **34**(5):423-429. [doi:10.1109/TCOM.1986.1096561]

Gardner, F.M., 1990. Frequency Detectors for Digital Demodulators via Maximum-likelihood Derivation ESA Final Rep: Part 2, ESTEC Contract 8022/88/NL/DG.

Huang, Z.J., Yi, Z.Q., Zhang, M., Wang, K., 2004. 8PSK Demodulation for New Generation DVB-S2 Communications, Circuits and Systems. ICCCAS 2004, **2**(27-29):1447-1450.

Hughes Network Systems, 2003. LDPC Frame Synchronization. DVB-S2-104.

Karam, G., Sari, H., 1995. A reduced-complexity frequency detector derived from the maximum-likelihood principle. *IEEE Trans. Commun.*, **43**(10):2641-2650. [doi:10.1109/26.469435]

Mengali, U., D'Andrea, N.A., 1997. Synchronization Techniques for Digital Receivers. Plenum Press, New York, USA.

Nemer, E., 2005. Physical Layer Impairments in DVB-S2 Receivers. Consumer Communications and Networking Conference, p.487-492.

Sun, F.W., Jiang, Y., Lee, L.N., 2004. Frame synchronization and pilot structure for DVB-S2. *Int. J. Satell. Commun. Network.*, **22**(3):319-339. [doi:10.1002/sat.793]

van der Wal, R., Montreuil, L., 1995. QPSK and BPSK demodulator chip-set for satellite applications. *IEEE Transactions on Consumer Electronics*, **41**(1):30-41. [doi:10.1109/30.370307]